Taylor & Francis
Taylor & Francis Group

Australian Journal of Earth Sciences

An International Geoscience Journal of the Geological Society of Australia

ISSN: 0812-0099 (Print) 1440-0952 (Online) Journal homepage: http://www.tandfonline.com/loi/taje20

HyLogger-3, a visible to shortwave and thermal infrared reflectance spectrometer system for drill core logging: functional description

M. C. Schodlok, L. Whitbourn, J. Huntington, P. Mason, A. Green, M. Berman, D. Coward, P. Connor, W. Wright, M. Jolivet & R. Martinez

To cite this article: M. C. Schodlok, L. Whitbourn, J. Huntington, P. Mason, A. Green, M. Berman, D. Coward, P. Connor, W. Wright, M. Jolivet & R. Martinez (2016): HyLogger-3, a visible to shortwave and thermal infrared reflectance spectrometer system for drill core logging: functional description, Australian Journal of Earth Sciences

To link to this article: http://dx.doi.org/10.1080/08120099.2016.1231133

AUSTRALIAN JOURNAL OF EARTH SCIENCES, 2016
http://dx.doi.org/10.1080/08120099.2016.1231133

HyLogger-3, a visible to shortwave and thermal infrared reflectance spectrometer system for drill core logging: functional description

M. C. Schodlok[a], L. Whitbourn[b], J. Huntington[b], P. Mason[b], A. Green[c], M. Berman[d], D. Coward[b], P. Connor[b], W. Wright[b], M. Jolivet[b] and R. Martinez[b]

[a]Federal Institute for Geosciences and Natural Resources (BGR), Geozentrum Hannover, B4.4 Geo-Hazard Assessment, Remote Sensing, Stilleweg 2, 30655 Hannover, Germany; [b]CSIRO Mineral Resources, PO Box 52, North Ryde, NSW 1670, Australia; [c]OTBC Pty. Ltd, Australia; [d]CSIRO Data61, PO Box 52, North Ryde, NSW 1670, Australia

ABSTRACT

Australian Geological Surveys are the custodians of a major national asset in the form of historically drilled and archived drill cores of the top few kilometres of the continent acquired by government agencies and companies over many decades. The AuScope National Virtual Core Library (NVCL) component of the AuScope Earth Model comprises geological/rock samples, technology, people and database/delivery infrastructure located in six nationally distributed nodes and is aimed at extracting additional value from this asset. The technology components of the NVCL comprise an integrated suite of hardware (HyLogger-3) and software (TSG-Core) systems for the imaging and hyperspectral characterisation of drill cores in their original core trays and the interpretation of their contained oxide, carbonate, hydrous and anhydrous silicate mineralogy. The HyLogger-3 includes state-of-the-art Fourier Transform Spectrometers that continuously measure calibrated spectral reflectance from nominal 10 by 18 mm fields of view. These spectra are in turn passed through a series of automatic and semi-automatic pre-processing and mineralogical unmixing algorithms. These, along with numerous other tools in TSG-Core, output a variety of mineralogical and image products for use by scientists in many branches of the earth sciences. This paper provides a functional overview of the HyLogging hardware and software tools available in each of Australia's Geological Surveys.

ARTICLE HISTORY
Received 8 April 2016
Accepted 9 August 2016

KEYWORDS
HyLogger; hyperspectral drill core logging; AuScope National Virtual Core Library (NVCL); reflectance spectroscopy; visible near infrared; short wave infrared; thermal infrared; The Spectral Geologist (TSG)

EDITORIAL HANDLING
Belinda Smith

Introduction

The acquisition of diamond drill core is almost always the most expensive single part of mineral exploration, and future exploration is increasingly moving under extensive cover where drilling will be more and more important (Australian Academy of Science, 2012). Furthermore, given additional investment by the oil and gas sector, state agencies engaged in industry facilitation, and companies in-mine development drilling, it is absolutely essential that as much additional information as possible is recovered and re-used to fuel future programs. As a result, new technologies are required to handle very large volumes of drill core, to extract as much information from the cores as possible in order to increase the effectiveness of traditionally time-consuming, expensive and labour-intensive conventional core logging. Conventional drill-core logging can also be very subjective and variable, particularly with hard-to-recognise bleached clay minerals and fine-grained materials, or if multiple geologists log holes across a single project. All this can lead to inconsistencies, misinterpretation of the mineralogy or even to missed minerals.

Reflectance spectroscopy offers a rapid, non-destructive and objective enhancement to conventional manual core logging. It provides mineralogical information about rocks based on diagnostic reflectance features related to the electronic and vibrational properties of their mineral components. Measurements in the visible to near infrared (VNIR), from 400 to 1000 nm,[1] and shortwave infrared (SWIR), from 1000 to 2500 nm, are used to characterise and analyse iron oxides, rare earth minerals, hydrous silicates, carbonates and some sulfates. Measurements in the longer wavelength, thermal infrared (TIR) region, from 6000 to 14 500 nm, respond to anhydrous silicates, including for example, quartz, feldspars, garnets, pyroxenes and olivines, as well as hydrous silicates, sulfates and carbonates. Barite and apatite are examples of other minerals that can also be sensed in the TIR region but not in the SWIR. To acquire all this information, CSIRO has developed the HyLogger-3^{TM} (Figure 1), a rapid automated drill core line-profiling system acquiring hyperspectral reflectance data that are co-registered with high-resolution digital imagery of the core.

A rapid, automated sensing system such as this needs appropriate interpretation and analysis software that can deal quickly with this type of hyperspectral data in large volumes. CSIRO has also developed 'The Spectral Geologist' (TSG^{TM}) software package that processes these data, from the quality control and data pre-processing stage through to final

CONTACT M. C. Schodlok martin.schodlok@bgr.de

Figure 1. One of the NVCL HyLogger-3 instruments. The spectrometers and control electronics are embedded in top section of the blue frame. Below that, the lighting system directs the illumination onto the calibration block at the beginning of the X–Y translation table. The data-acquisition system, X–Y table controller and power supply unit are in the blue frame under the X–Y table.

product stages, for example mineral distributions and abundances down the drill hole. TSG includes tools for the extraction of diagnostic mineral features for core characterisation as well as spectral unmixing methods for mineralogical identification of mixed spectra from the VNIR–SWIR and the TIR, as demonstrated in several studies (see this volume and Haest et al., 2012a, 2012b; Huntington et al., 2006; Roache et al., 2011; Thompson et al., 2008).

HyLogging Systems, comprising HyLogger-3 hardware and TSG-Core software, have been distributed to the geological surveys of the Australian states and territories under the umbrella of the AuScope and CSIRO funded National Virtual Core Library (NVCL). These systems have been in routine operation scanning drill cores on a daily basis around Australia, with TIR capability, since 2010. This paper provides a functional description of this system and gives some examples of typical outputs of the current HyLogger-3 and TSG capabilities.

Instrument description

The HyLogger-3 makes measurements by robotically translating core trays on an X–Y table beneath stationary sources and spectrometer systems. The sources illuminate the core beneath two collection telescopes that are displaced parallel to the direction of translation of the core. The first collects reflected light in the VNIR and SWIR, and the second in the TIR. The spectrometers are complemented by a camera to image the core and a laser-based height measurement system (profilometer) to acquire the profile of core height along the core. These four discrete measurement systems are spaced 100 mm apart, in the direction of travel of the core tray. The software that controls the instrument assembles co-registered data, including a camera image, for successive measurement positions, which are spaced at 4 mm intervals along the direction of travel. Various standard targets are mounted on the X–Y table for regular calibration checks, as described below.

The measurement geometry for both the VNIR/SWIR and TIR is illustrated in Figure 2. Dual sources (S) illuminate the mineral sample (M), and the reflected radiation is collected through a telescope (T) into the monochromators and interferometers of the detection system (D). Calibration targets (C) are moved under the system as required. The angle of incidence (I) for both sources is approximately 20°.

The illumination for the VNIR/SWIR system is provided by a pair of quartz-halogen lamps disposed along the direction of

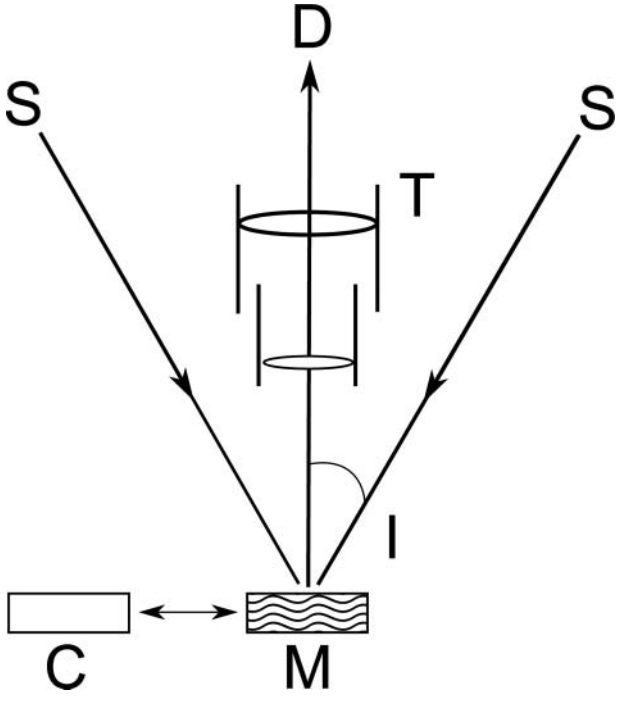

Figure 2. Schematic diagram of the illumination sources, telescopes, target samples and calibration targets.

travel of the core. The TIR sources are heat sources at the foci of aluminium parabolic mirrors. These direct thermal radiation from a 800°C blackbody source onto the target.

The VNIR/SWIR detection system is composed of a grating spectrometer with a silicon array detector for the VNIR and a rapid scan Fourier Transform Infrared (FTIR) spectrometer with a single-element liquid-nitrogen cooled InSb detector for the SWIR. A beam splitter separates these components from the common telescope. The separately acquired VNIR and SWIR spectra are later merged into a single VNIR–SWIR spectrum. The TIR is measured with a separate telescope and associated FTIR spectrometer with a single-element liquid-nitrogen-cooled MCT (mercury cadmium telluride: HgCdTe) detector. The outputs of the two systems (VNIR/SWIR and TIR) are spatially registered as part of the data processing, to an accuracy of approximately ±1 mm. The 10 mm-diameter instantaneous field of view of the spectrometers is spread along track by X–Y table motion, resulting in an overall field of view of 10 mm × 14 mm for a single spectrum, and more commonly 10 mm × 18 mm, when successive pairs of spectra are averaged in post-processing of the data. Overall specifications of the various HyLogger-3 sensors are given in Table 1.

Measurements of reflectance calibration targets (C in Figure 2) are performed at the beginning of each tray scan to provide reproducible reflectance measurements. To avoid accelerated deterioration of the primary standards, transfer targets are used for routine core tray measurements. These are a panel of white PTFE for the VNIR–SWIR and a panel of uncalibrated Infragold® in the TIR. In each case, the relative reflectance of the transfer target ρ_t is measured by regular comparison with a corresponding primary reflectance standard using the HyLogger in its standard double-bidirectional mode. These relative reflectances are corrected to directional hemispherical reflectances using the NIST-traceable reflectance data supplied with the primary standards. The primary standards are a Labsphere Spectralon® reflectance standard for the VNIR–SWIR reflectance measurements and a Labsphere Infragold® reflectance standard for TIR reflectance measurements.

TIR calibration also requires measurement of the background radiance, which is performed by moving a 'background mirror' into the field of view of the TIR telescope in order to measure room radiance (background temperature). To allow the TIR background data to be calibrated to radiance, the system is also calibrated at the beginning of each operating day by measurement of two black bodies at different temperatures.

Sample preparation for HyLogging is usually limited to cleaning the core to remove dust, powders, leaves and other core tray rubbish. As with all reflectance spectroscopy, core samples must be dry. During each scan the drill core is translated at 48 mm/s, reversed for alternate tray sections, with added time required for loading and unloading and the calibration cycle, etc., leading to an overall scanning rate of about 1 m per minute, allowing up to 500 m of core to be scanned in an 8-hour shift.

The HyLogging system is equipped with a diagnostics version of The Spectral Geologist software (TSG-QC) to monitor performance and data quality. This software processes the acquired data immediately after each tray is scanned and assesses system performance, based on carefully defined thresholds. Errors are flagged by labels on an image of the core tray, which is generated and displayed automatically at the end of each scan, along with a preliminary mineralogical interpretation of the spectral reflectance data. This enables the operator to confirm data quality before loading the next core tray. The TSG-QC operation typically takes 20–50 s, depending upon tray size.

Data processing

The system response in all three wavelength regions is sufficiently linear that simple corrections for scale and offset are all that is necessary to convert the data to reflectance. If V is the system response to the target, V_t the response to the transfer standard and V_b a background response, then the base reflectance of the target, $\hat{\rho}$, is then calculated as

$$\hat{\rho} = \rho_t \frac{V - V_b}{V_t - V_b} \tag{1}$$

where

$$\rho_t = \rho_s \frac{V_t - V_b}{V_s - V_b} \tag{2}$$

is the NIST-traceable directional hemispherical reflectance of the transfer target measured relative to that of the primary reflectance standard, V_s, using the measurement

Table 1. Specifications of the three HyLogger-3 spectrometer systems.

Parameter	VNIR	SWIR	TIR
Spectral range	380–1000 nm	1000–2500 nm	6000–14 500 nm
Channels	156	376	341
Wavelength sampling	4 nm	4 nm	25 nm
Spectral resolution	4 nm	4 nm from 1000 nm to 1600 nm, rising to 10 nm at 2500 nm	25 nm at 6000 nm, rising to 120 nm at 14 500 nm
Spatial resolution (field of view)	10 mm across track × 14 mm along track @ 4 mm sampling interval 10 mm across track × 18 mm along track @ 8 mm sampling interval		
Peak SNR[a]	2000 @ 1000 nm	≥ 2000 @ 2500 nm	≥ 2000 @ 8 μm
Margin SNR	500 @ 380 nm	≥ 500 @ 1000 nm	500 @ band ends
Profilometer height resolution	0.25 mm		
Profilometer sampling interval	0.0625 mm (16 points/mm)		

[a]SNR: signal-to-noise ratio for Lambertian target with directional hemispherical reflectance of 100%.

configuration shown in Figure 2, where all of these quantities are functions of wavelength.

All sample reflectance measurements are therefore a double ratio with the effect that the diffuse reflectance properties of the transfer standards cancel out, and the measured mineral reflectances are referred to the NIST-traceable directional hemispherical reflectance data of the primary standards. Band-specific aspects of the process are addressed in the relevant sections below.

There is also one important generic nuance in all these reflectance measurements. To the extent that the primary reflectance standard and the measured mineral target are Lambertian (i.e. perfectly diffuse) reflectors (or alternatively, that they both have identical scattering properties) and that both are horizontal and equidistant from the (downward looking) spectrometer telescope, the double bi-directional reflectance measured by the VNIR/SWIR and TIR spectrometers in the HyLogger is in units of absolute directional hemispherical reflectance equivalent to that supplied by the manufacturer of the primary standard (i.e. Spectralon® in the VNIR–SWIR range and Infragold® in the TIR range). In general, however, real drill core targets are neither Lambertian, nor flat, nor horizontal, nor at exactly the same distance from the telescope (and illumination sources) as the reflectance transfer standard. So, provided that the primary reflectance standard is Lambertian, the system measures the directional hemispherical reflectance of a Lambertian reflection target, which, if placed in the same position as the target, would produce the same reflected signal as the mineral target being measured, in the double-bi-directional reflectance geometry of the HyLogger. We call this *the equivalent directional hemispherical reflectance of the target*.

For the VNIR spectrometer, V_b is measured by measuring the signal from the spectrometer when its input aperture is blocked by a black shutter. The SWIR spectrometer has an alternating current coupled signal path, which is not subject to a drifting baseline. Measurements of the background signal, V_b, show that it is less than the noise from the SWIR spectrometer in the absence of any source radiation. Accordingly, we use $V_b = 0$ in the SWIR.

The TIR measurement incorporates a strong background signal in addition to the reflected source signal. This background signal is the sum of radiation emitted by the target plus blackbody radiation from the environment that is reflected by the target. This must be subtracted in order to give valid reflectance measurements. The orientation of the background mirror providing V_b is selected so that the source radiation is directed towards a distant point, ensuring that the incoming radiation is dominated by the background room radiation.

If the temperatures of the room, all HyLogger surfaces and the mineral target were all the same, the TIR background signal would be identical to that seen from the target itself, and then Equation 1 would deliver the calibrated *equivalent directional hemispherical reflectance of the target* in the same way as the VNIR and SWIR spectrometers, i.e. $\hat{\rho}$ would be a good estimate of ρ, the true reflectance of the sample. In practice, there are finite temperature differences between target, room and instrument, and this introduces errors in the measured reflectance. For that reason, we call the reflectance measured by the TIR spectrometer *TIR base reflectance*.

When the sample temperature is different from that of the background, it can be shown that

$$\hat{\rho} \approx \rho + Q(\Delta T) \tag{3}$$

where ρ is the true reflectance of the target, ΔT is the temperature difference between the sample and the background, and $Q(\Delta T)$ is a pseudo-reflectance curve that is determined as part of the calibration process. This curve adds an overall background to the spectrum that increases as the temperature difference between the core and the room increases. This relation can be used in later processing to correct the data when there has not been time for the core tray to equilibrate with the room temperature before measurement and/or to correct for heating by the scanning of adjacent sections of the tray. In general, this correction procedure works satisfactorily for ΔT values in the range of $\pm 10^{\circ}$C. The temperature differences involved are generally somewhat less than that.

Spectral reproducibility

The reproducibility of spectral data from the HyLogger-3 is important for reliable mineralogical interpretation and consistent results from multiple data sets over time. To assess the reproducibility of the system, the same quartz sample was measured 79 times during a period of three months. The upper plots in Figure 3 show the mean and ± one-standard-deviation spectra for the VNIR–SWIR (left) and TIR (right). The lower plots show normalised versions of the same spectra.

In the VNIR–SWIR the ±1-standard-deviation spectra show a maximum variability in reflectance of 0.03, while in the TIR the corresponding variability is about 0.01. Normalisation of the spectra reduces this to less than 0.01 in both ranges, showing that the shapes of the spectra measured by the instrument are highly reproducible.

The wavelength calibration of the VNIR–SWIR is very accurate, with variation in the wavelength position of selected features of less than ±1 nm across the 400–2500 nm range. In the TIR, these data showed exceptional reproducibility of ± 0.2 nm at the mineral diagnostic quartz feature at 8627 nm (8.827 μm). In general, however, the TIR wavelength calibration is observed to be within ±1 nm at 6000 nm, rising to about ± 5 nm at 14 500 nm based on observations of absorption features in polystyrene plastic.

Data interpretation

The spectroscopic and image data collected by the HyLogger-3 can be processed and analysed using the TSG-Core version of 'The Spectral Geologist (TSG™)' software (see www.thespectralgeologist.com). TSG provides many tools for characterisation, feature extraction and mineral identification using all wavelengths of HyLogging data in association with its core

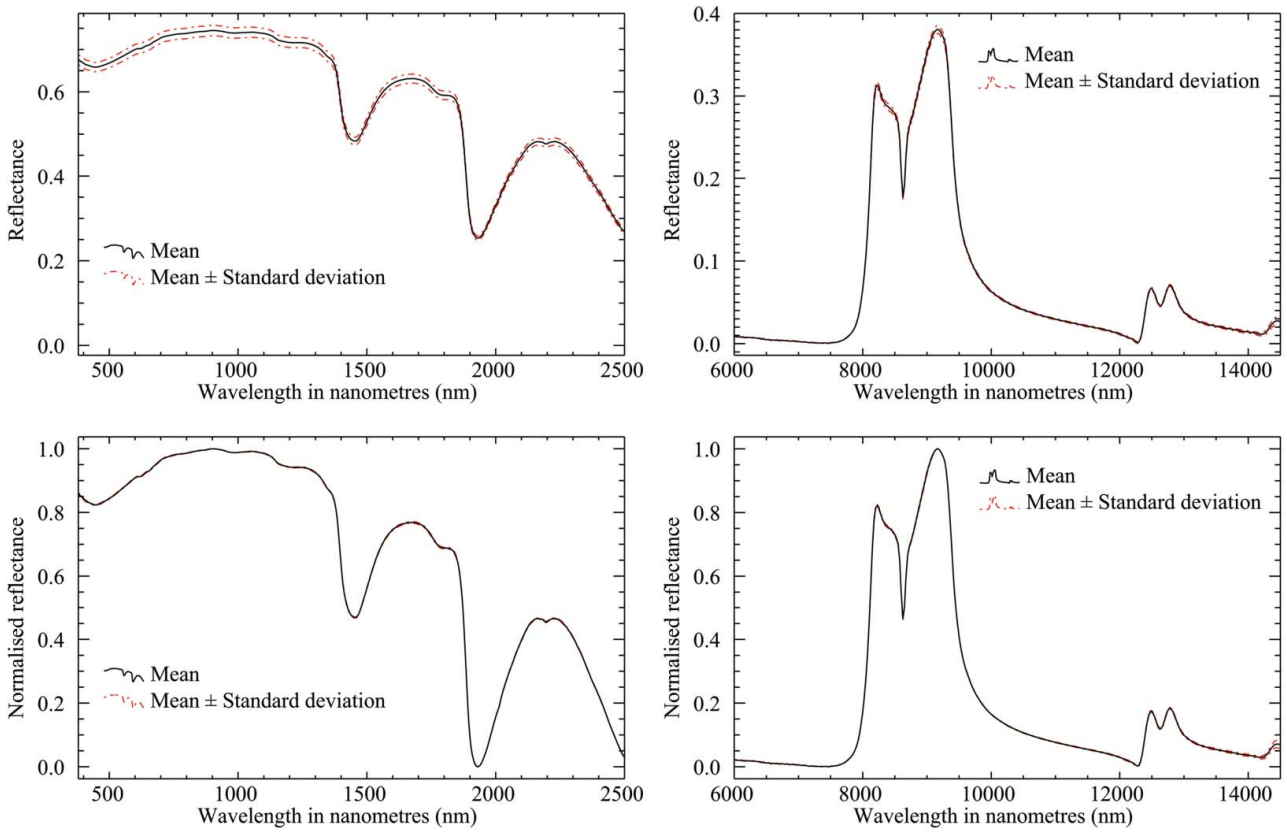

Figure 3. Mean and ± 1 standard-deviation HyLogger-3 spectra for 79 quartz data sets acquired during a period of three months. Left (a) VNIR–SWIR and right (b) TIR spectra. Normalised spectra (lower plots) show very high reproducibility in spectral shape. Wavelengths are shown in nanometres (nm). 1000 nm = 1 micrometre or micron (μm).

images. The images are used for visual validation to minimise ambiguities and possible misinterpretation owing to, for example, broken core. Tools also exist to create ENVI[2] readable spectral libraries, although without any of the associated HyLogging reference and image data.

The interpretation of the HyLogged spectra involves two related problems. The first is to decide what minerals are present in the rock and the second is to estimate their abundances.

These two problems may be tackled in two or three ways, as described below. Initially, methods exist that are essentially interactive and exploratory in nature and are used by expert interpreters to investigate individual spectra or to characterise the downhole distribution of selected minerals or mineral chemistry variations.

For example, sometimes the presence of a mineral can be determined by the identification of one or two unique features in the spectrum, although this does require some knowledge of mineral absorption features. If these features persist when the mineral occurs in reasonable abundance and are not distorted by overlapping features from other minerals present in the IFOV[3] of the HyLogger, they can be used with confidence. TSG offers a number of procedures to measure the characteristics (usually wavelength position and depth) of such features. In TSG such characteristics, spectral parameters or indices are called scalars. The most important of these scalars, PFIT uses a polynomial fit of user-selectable order 2 to 12 and a local least-squares fit to estimate wavelength position and depth. With these procedures, absorption feature depths are considered a surrogate for relative mineral abundance and wavelength a surrogate for mineral composition (e.g. Duke, 1994; McLeod et al., 1987; Scott et al., 1998). Some typical examples that can be shown to correlate with mineral composition include the 2210 ± 20 nm for white micas, the 2257 ± 10 nm for chlorites, biotite or phlogopite and the 6500 nm peak for carbonates in the TIR.

When a mineral spectrum is largely not compromised or distorted by features of other minerals, a simple correlation measure against some reference spectrum may also be useful for identification. TSG's AuxMatch correlation procedure, suitably thresholded, can be used in these circumstances.

Most importantly, TSG also offers methods, described below, for fully automatic mineral mapping that are critical for preliminary analysis of large HyLogging data sets comprising tens or hundreds of thousands of spectra, where the operational focus is on mineralogical products, not individual spectra.

Central to TSG's processing philosophy is geological context. This means that, wherever possible, testing for minerals or mineral groups is restricted to those thought likely to be present in a region, province or dataset. TSG draws on several quite large (although not all-encompassing) spectral libraries, but if studying a sedimentary basin, with no basement, it is unlikely to encounter olivine, for

example, in sufficient quantity to be identified (unless in fresh dykes or sills). In such instances, TSG provides tools to build and save an 'active minerals list' for the region, province or dataset and in this way minimise erroneous identifications caused by noise or the complexities of choosing from many possible mixtures.

Once the correct set of minerals has been identified, estimating abundances can proceed by modelling the spectrum as a linear mixture of the spectra of the constituent minerals plus some extra (usually smooth) modelled curves to account for variations in background. In the VNIR/SWIR regions, where light is reflected by volume scattering mechanisms, the data are first transformed with a logarithmic transform (a good approximation to the Hapke transform; Hapke, 2012) before the modelling. After this transformation, the mixing of the constituent mineral spectra is approximately linear. In the TIR, where surface scattering mechanisms dominate reflectance (Thompson & Salisbury, 1993), no preliminary transformations are necessary.

TSG offers two automated unmixing methods, The Spectral Assistant (TSA^{TM}) and Constrained Least Squares (CLS).

TSA^{TM} combines the identification and abundance estimation stages mentioned above (Berman et al., 1999, 2011). The constituent minerals are chosen by a fast subset selection algorithm (Miller, 2002) in combination with the linear modelling procedures discussed above. The subset selection procedure searches among all the possible linear combinations of 1, 2 or 3 reference mineral spectra (with positive weights) for the combination that best fits a given unknown spectrum. For example, starting with the current SWIR library of 60 reference spectra and seeking the three mineral spectra that, in linear combination, best model an unknown spectrum, TSA searches through singletons, doubles and all 34 220 possible combinations of three spectra, and returns the mixture of up to three minerals with positive weights that best satisfies a defined measure of fit.

The measure of fit used by TSA depends on the wavelength region. In the VNIR and the SWIR, it is a Mahalanobis distance (De Maesschalck et al., 2000) (referred to as the SRSS or standardised residual sum of squares), where the residuals to the fit are rescaled by an estimate of a consolidated within-class covariance matrix. Mahalanobis distance has minimum classification error under idealised assumptions (McLachlan, 1992). This is reflected in TSA in the VNIR and SWIR, where use of Mahalanobis distance correctly identifies minerals in mixtures much more often than Euclidean distance does. In the TIR (for reasons discussed below) the measure of fit used is a simple Euclidean distance of the residuals.

The TSA algorithm takes the results of the subset selection procedure and applies a set of rules that reject unsatisfactory combinations of spectra and samples where results are unreliable. These rules reject samples that have very low signal-to-noise ratios, are very dark or have estimated mineral proportions that are less that can be justified by the quality of the data.

In order to model adequately the full range of spectra that can be encountered in HyLogger data, it is necessary to have access to a wide range of representative spectra of pure minerals. In general there can be more than one spectrum associated with each mineral. In the SWIR this apparent replication arises from the need to be able to model chemical variability within solid solution series. The availability of a range of spectra for individual minerals (e.g. muscovites, Fe-chlorites) enables us to estimate the consolidated within-class covariance matrix used to calculate a Mahalanobis distance (see above). Similar considerations apply in the TIR, but there is further variability owing to crystallographic orientation and surface condition effects.

Orientation effects arise because the shape of reflectance spectra of low-symmetry crystals in the TIR can vary markedly with measurement geometry. In the analysis of drill core, there is no opportunity to process and homogenise samples in a way that would average out these orientation effects, so it is necessary to have enough reference spectra to model adequately surfaces that could be seen on normal drill core. Unfortunately, currently we do not have enough TIR reference spectra to model this variability, so Euclidean distance is used instead of Mahalanobis distance.

Surface condition is important for TIR reflectance because, as the surface is roughened or clinging fines coat the surface, volume scattering becomes important, and the nature of the reflectance changes. To a certain extent, these changes can be accommodated within the linear model by incorporating extra spectra in the model, but when volume scattering begins to dominate the spectrum and significantly changes the spectral characteristics, unmixing the TIR spectra becomes very problematic.

TSA selects from a set of 60 spectra in the SWIR and 141 spectra in the TIR. The minerals that are currently available to TSA are shown in Table 2. New minerals are being added as required.

When a new drill hole is first encountered and scanned with the HyLogger, the drill hole's context for the creation of a relevant *active minerals list* may not be known, and so TSA must use the full suite of minerals. This initial interpretation, which takes place very rapidly per core tray on the HyLogger itself, produces a set of unmixing results referred to as the System Set or sTSAV in the VNIR, sTSAS in the SWIR and sTSAT in the TIR. As soon as possible after completing logging a hole, an analyst may examine the data, develop some mineralogical context (i.e. turn off some minerals, based on spectroscopic and geological expert knowledge) or load a pre-saved *active mineral list* for the deposit. At this point TSA re-runs, now on a shorter list of minerals, and produces a second, more refined/reliable interpretation referred to as the User Set (uTSAV, uTSAS and uTSAT). Both System and User results are kept and may be compared or the User TSA re-run with a still more refined active minerals list. Typically, only the User results are published.

In the SWIR and VNIR, TSA executes quite quickly when searching for mixtures of two or three spectra. Also, because it is relatively uncommon for more than this number of reference spectra to be necessary to model a single SWIR spectrum, sTSAS and uTSAS can provide a reasonable guide to the unknown mineralogy in quite acceptable time. This is less true for TIR spectra.

Table 2. Main minerals and mineral groups the HyLogger-3 and TSG-Core have been able to detect.

VNIR Groups
Iron Oxide Group Minerals
Hematite, goethite, jarosite, massive magnetite
Rare Earth Element bearing minerals
Monazite-Nd, Bastnasite-Nd, etc.
SWIR Groups
Al(OH) Group Minerals
Paragonite, muscovite, phengite, illite, pyrophyllite, kaolinite, halloysite, dickite, smectite varieties, gibbsite, diaspore, gibbsite, prehnite, palygorskite, etc.
Sulfate Group Minerals
Na and K alunites, jarosite, gypsum, epsomite, goslarite, etc
Si(OH) Group Minerals
Opaline silica and hydrothermal quartz with fluid inclusions
Ammonium-bearing minerals
NH-alunite, buddingtonite, Na illite, etc.
Fe(OH) Group Minerals
Saponite, nontronite
Mg(OH) Group Minerals
Chlorites (Mg/Fe), biotite, phlogopite, antigorite, tremolite, actinolite, talc, hornblende, brucite, etc.
Carbonate Group Minerals
Calcite, dolomite, Fe-dolomite, magnesite, ankerite, siderite, malachite, other Cu carbonates, etc.
Selected OH-bearing Silicates
Epidote, clinozoisite, zoisite, tourmaline, topaz, etc.
Zeolites Group Minerals
Laumontite, natrolite, chabazite, etc.
Selected massive sulfides
Sphalerite
Others
Kerogen, bitumen
Non-geological materials
Various core tray plastics, cellulose (wood)
TIR Groups
Silica Group Minerals
Quartz, opal
Potassium Feldspar Group Minerals
Orthoclase, microcline, anorthoclase
Plagioclase Feldspar Groups Minerals
Albite, oligoclase, andesite, labradorite, bytownite, anorthite
Pyroxene Group Minerals (clino- and ortho-pyroxenes)
Augite, diopside, hedenbergite, enstatite
Olivine Group Minerals
Forsterite, fayalite
Garnet Group Minerals
Andradite, grossular, almandine, spessartine, uvarovite
Serpentines
Lizardite, antigorite
Sulfates
Anhydrite, barite, plus all the SWIR active sulfates
Carbonates
Rhodochrosite, plus all the SWIR active carbonates
Phosphates
Apatite
Borates
Vonsenite
Oxides
Magnetite, hematite, goethite, ilmenite, rutile, gahnite, etc.
Miscellaneous silicates
Zircon, vesuvianite
Metamorphic silicates
Andalusite, cordierite, kyanite, sillimanite, staurolite

In the TIR, because both the hydrous and anhydrous minerals respond, four or five minerals (sometimes more) are commonly needed to model a given spectrum. In addition, the orientation and surface condition effects mean that the subset selection procedure has to search for these larger subsets within a reference set of many more spectra than in the SWIR. SWIR searches involve a few thousand alternative combinations of spectra, whereas typical TIR searches can involve half a million alternative combinations, and this without assurance of finding all the important spectra for a typical multi-mineralic rock. These limitations mean that sTSAT, and even uTSAT, execute longer for a less reliable result than sTSAS/uTSAS.

To overcome this limitation TSG offers another method to model TIR data that allows more spectra to be included in the fit. The CLS procedure (commonly called non-negative least squares by mathematicians; Lawson & Hanson, 1995) fits spectra in a user-specified sub-library subject to the constraint that they are included with non-negative weights. The CLS is implemented using a quadratic programming algorithm (Nocedal & Wright, 1999).

While CLS overcomes important limitations of TSAT, it must be used with great care because it will always overfit if too many spectra are offered to it, resulting in errors of commission. For this reason, it must be used in situations where a knowledgeable user selects the assemblage of minerals to be included in the fit. This can be done when interpreting single spectra or segments of the drill hole referred to as domains.

TSG allows the user to partition the hole into spatially continuous domains, which are assumed to be characterised by a single mineral assemblage called a Restricted Mineral Set (RMS). Once an RMS has been defined for a domain, both TSA and CLS can be constrained to model the data using only the spectra associated with the chosen minerals. Although it was introduced to improve TIR unmixing, this strategy applies to modelling in all three wavelength regions. When TSA is run with this user-selected RMS, it is known as domain-TSA (dTSA).

Both TSA and CLS execute much faster when working with smaller numbers of reference spectra and, if the RMS has been selected correctly, the possibility of errors of commission is greatly reduced. In general, if the data were well modelled by a sensible set of spectra, it is reasonable to expect that the proportions are then realistically estimated. However, it must always be remembered that linear modelling can sometimes produce non-unique results when the problem is undetermined (Menke, 1989). This non-uniqueness is most common when the spectrum of the unknown sample is weak (e.g. dark, opaque or reflect low mineral abundance) with poorly defined features and when the features that are present can be caused by more than one mineral.

Figure 4 shows the spectral characteristics in the VNIR–SWIR (left) and TIR (right) of quartz, plagioclase, kaolinite, actinolite, calcite, goethite and gypsum measured with the HyLogger-3. This plot also demonstrates the obvious differences in the characteristics of the spectra within both wavelength ranges. The VNIR–SWIR spectrum is dominated by volume scattering, resulting in absorption features. In contrast, the TIR is generally dominated by surface scattering, resulting in reflectance peaks or Reststrahlen bands (Salisbury & Wald 1992, Salisbury et al., 1991). Both wavelength ranges can be used to differentiate within mineral groups as well as between them, for example, phyllosilicates, inosilicates,

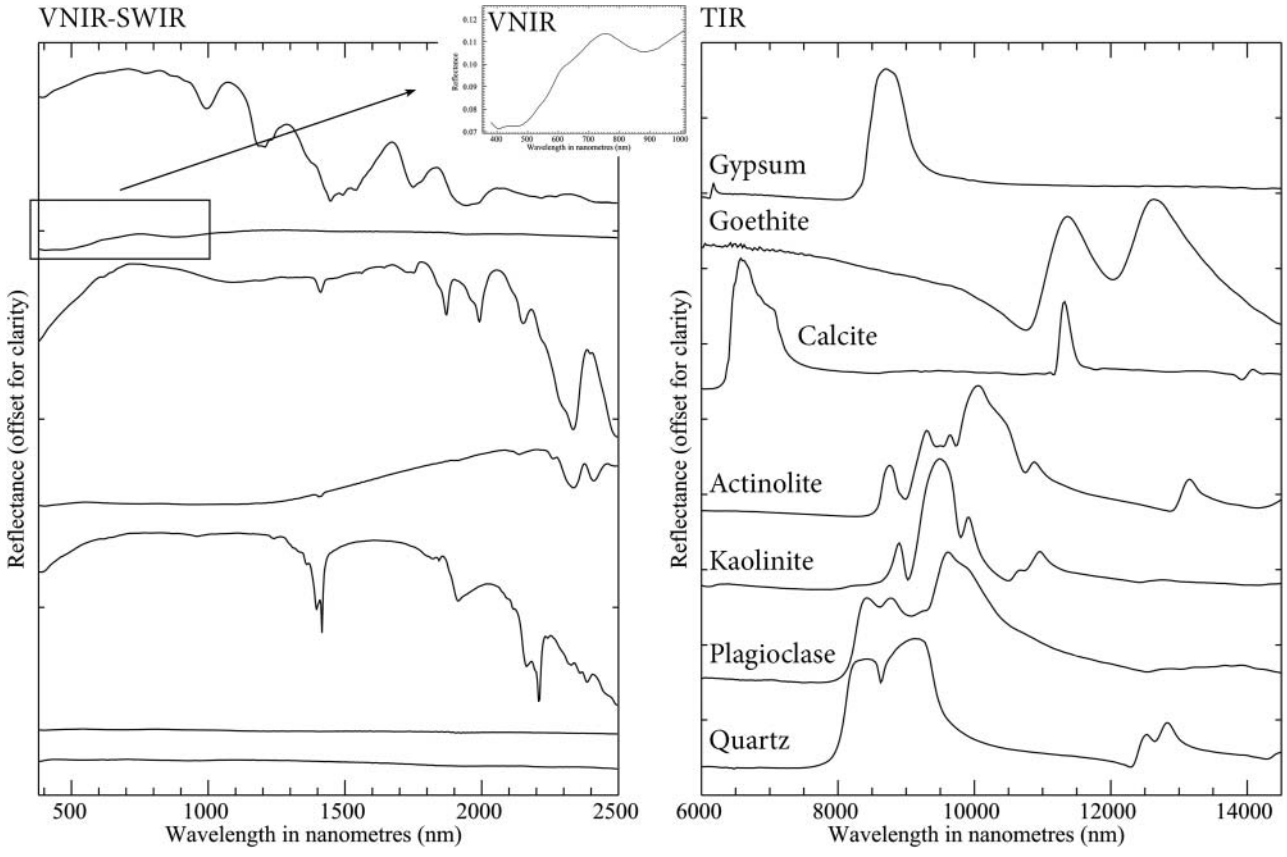

Figure 4. HyLogger-3 spectra of gypsum, goethite, calcite, actinolite, kaolinite, plagioclase and quartz in the VNIR/SWIR (left) and the TIR (right). Note that the VNIR/SWIR spectral features are generally absorptions whereas the TIR spectral features are generally reflectance peaks.

carbonates or sulfates. However, anhydrous silicates such as quartz and feldspars can be detected only and unambiguously using the TIR (Figure 4 right). Their diagnostic mineral spectral features lie between 8000 and 11 000 nm and not within the VNIR–SWIR.

Table 2 shows the mineral identification capability of the different wavelength regions for the HyLogging system (hardware and software) for common rock forming and alteration minerals or mineral groups. The list has been derived from hundreds of analysed drill cores and demonstrates the synergy gained by using the whole wavelength range to enhance the range of mineral identification. This is indicated for example by phyllosilicates such as micas, clays or chlorite that are more distinguishable in the SWIR, whereas the detection and estimation of relative abundances of carbonates is significantly improved by the TIR.

An important and useful characteristic of TIR spectra is the systematic shift of the major reflectance feature of silicates from shorter to longer wavelengths owing to the degree of polymerisation of the Si–O_4 tetrahedra, since higher bond strengths result in higher frequencies of vibrations (Salisbury et al., 1991). This introduces a feature, in a wavelength domain, of minimum reflectance and absorption, where the refractive index of silicates approaches 1. This minimum is called the Christiansen Feature (CF) and is driven by anomalous dispersion at shorter wavelengths from the Si–O bond stretching vibration. It can be correlated with the SCFM (silicon–calcium–iron–magnesium) chemical index SCFM = $SiO_2/(SiO_2 + CaO + FeO + MgO)$ of Salisbury and Walter (1989). This feature can be used to determine whether a rock or its constituent minerals is/are more silicic (shorter wavelengths) or more mafic or ultramafic (longer wavelengths), as shown in Figure 4 (right) by the shift from 7600 nm for quartz to 8500 nm for actinolite.

A closely related and empirical method developed for HyLogging uses the Felsic Mafic Index, the wavelength of the low-order maximum of the thermal infrared reflectance peak between 7800 and 12 000 nm for all minerals except carbonates. Figure 4 also illustrates how this wavelength maximum moves from left to right for the lowest four spectra with increasingly mafic mineralogy. In most practical instances, this has been found to be more discriminatory than the CF in describing calc-silicate and skarn-bearing terrains and is less impacted by distortions owing to volume scattering.

Hyperspectral drill core logging application

This section briefly illustrates the types of output from the HyLogger-3, resulting from the logging of a drill hole from the Dargues Reef gold deposit near Braidwood, New South Wales (Reid & Clissold, 2010). Reid and Clissold (2010), who initially examined the HyLogging data, describe Dargues Reef as a sulfide-rich, mesothermal, gold deposit, hosted in altered Braidwood Granodiorite, an early Devonian, metaluminous,

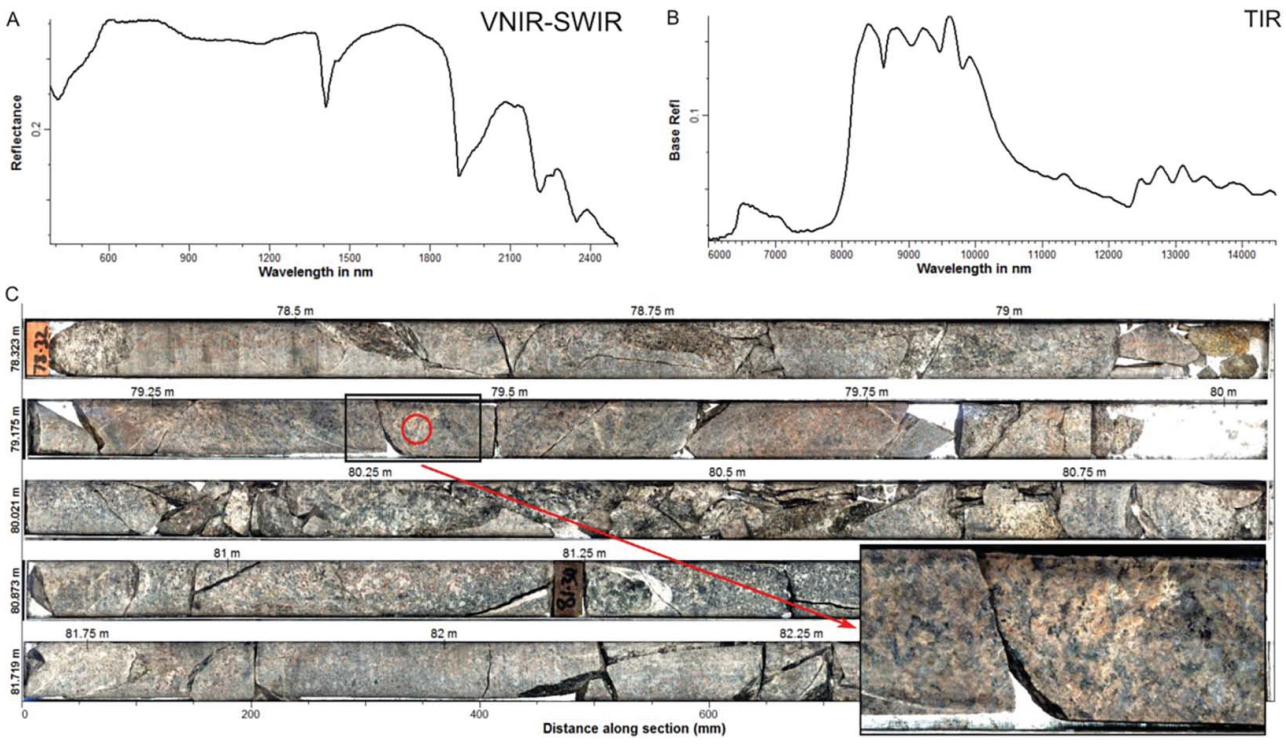

Figure 5. Typical HyLogger-3 outputs combining a single sample VNIR–SWIR spectrum (A top left), its companion TIR spectrum (B top right) and a core tray image (C) with a detailed image (bottom right) of the location corresponding to the spectra.

unfractionated I-type granodiorite. The granodiorite is typically equigranular with 15% biotite, chlorite and primary hornblende in its western phase. Propyllitic (distal) and phyllic (localised, proximal) alteration occur up to 80 m from mineralisation. Fluid temperature estimates of the deposit range from 350 to 380°C and are magmatic. Minor lower temperature minerals, e.g. prehnite and montmorillonite, are the final alteration product (Reid & Clissold, 2010).

The VNIR–SWIR spectrum in Figure 5 shows four major absorption features at 1400, 1900, 2200 and 2300 nm. The features at 1400 and 1900 nm (1.4 and 1.9 μm) are due to OH and H_2O. The features in the 2200 and 2300 nm regions result from combination bands owing to Al–OH and Mg–OH vibrations present in muscovite and chlorite. Additionally, the TIR spectrum indicates the presence of carbonate by the broad peak at around 6500 nm and the weak peak at 11 340 nm.

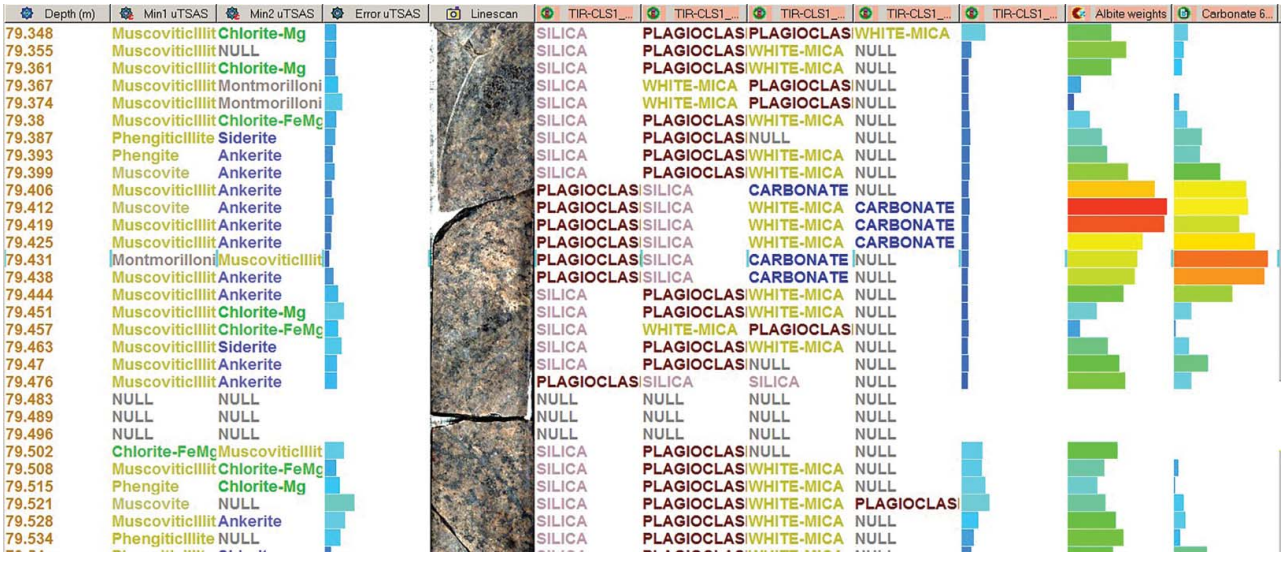

Figure 6. Per-sample log screen plot of the interval incorporated in Figure 5. The plot illustrates some of the options resulting from the semi-automated unmixing of tens of thousands of spectra. Depth (column 1) is followed by the dominant minerals in the SWIR (columns 2 and 3), their goodness of fit as determined by the TSA algorithm (column 4). These are followed by the linescan image, then the four dominant TIR mineral groups and their goodness of fit as determined by the domained CSL algorithm. The final two columns show the spectral proportions (weights) of albite and carbonate, respectively.

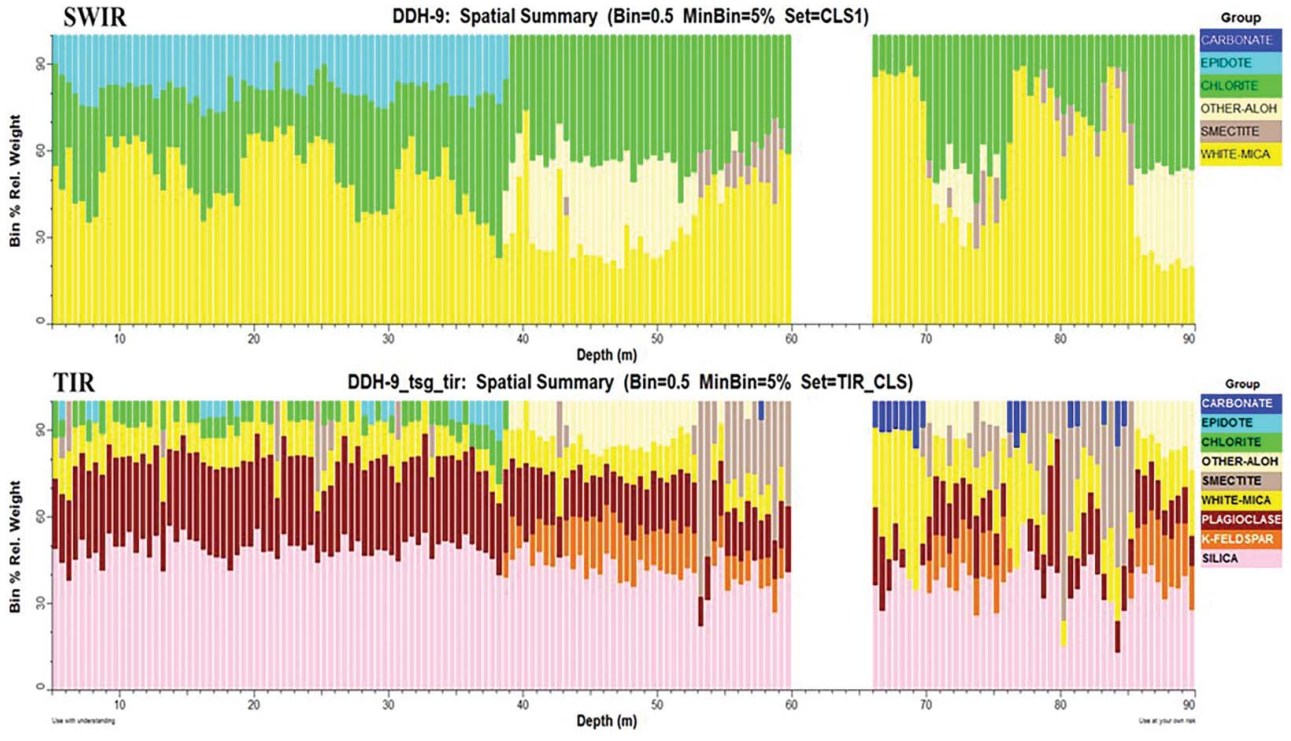

Figure 7. Summary mineral group interpretation for the entire DDH9 Dargues Reef drill hole using the CLS algorithm based on restricted mineral sets (RMS) for each spectro-mineralogical domain. Histogram intervals show normalised proportions per 0.5 m and do not show the lowest 5% of constituent mineral groups in each interval. The group Other AlOH includes the mineral prehnite.

The wavelength position of the latter peak can be used to identify the carbonates (Lane & Christensen 1997). The absorption feature at 8625 nm (between the two reflectance peaks) is a diagnostic indicator of quartz, which is also confirmed by a less intensive peak doublet at 12 500 and 12 750 nm. The double peak at 9600 and 9900 nm in combination with the absorption at 9800 nm as well as the four weak peaks beyond 12 750 nm indicates the sodium-rich plagioclase albite. In this instance, the phyllosilicates detected in the SWIR wavelength region are difficult to see in the TIR because their spectra are superimposed upon those of the more dominant framework silicates. Only spectral unmixing methods can reveal small amounts of those constituents from the TIR spectrum of the rock. The integration of multiple wavelengths with the HyLogger-3 thus permits the following visual estimate of the total mineral make-up of the example sample: from the TIR—quartz, albite, calcite and from the SWIR—muscovite and chlorite.

The results of semi-automatic data analysis using the unmixing methods mentioned above can be presented either as per sample results in a log column format (Figure 6) or as a spatial overview of the whole drill hole (Figure 7).

Figure 7 shows a drill hole summary of SWIR minerals (top) and TIR minerals (bottom) and illustrates that the drill hole can be separated into two domains with the boundary at a depth of about 40 m. The first domain is dominated by quartz, plagioclase, chlorite, with micas and epidote in low abundance. The second domain is still dominated by quartz, but the abundance of plagioclase has changed and intervals of K-feldspar and prehnite appear. A similar pattern is present for the phyllosilicates. In the first domain chlorite and white mica are dominant but in the second domain intervals of smectite

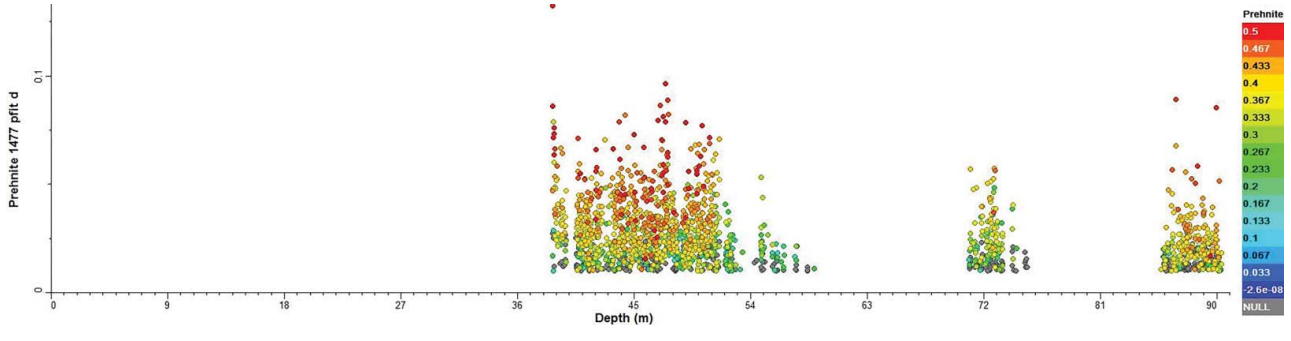

Figure 8. Per sample plot of the absorption depth, centred on 1477 nm, used as a surrogate for abundance, of prehnite, a common derivative of plagioclase.

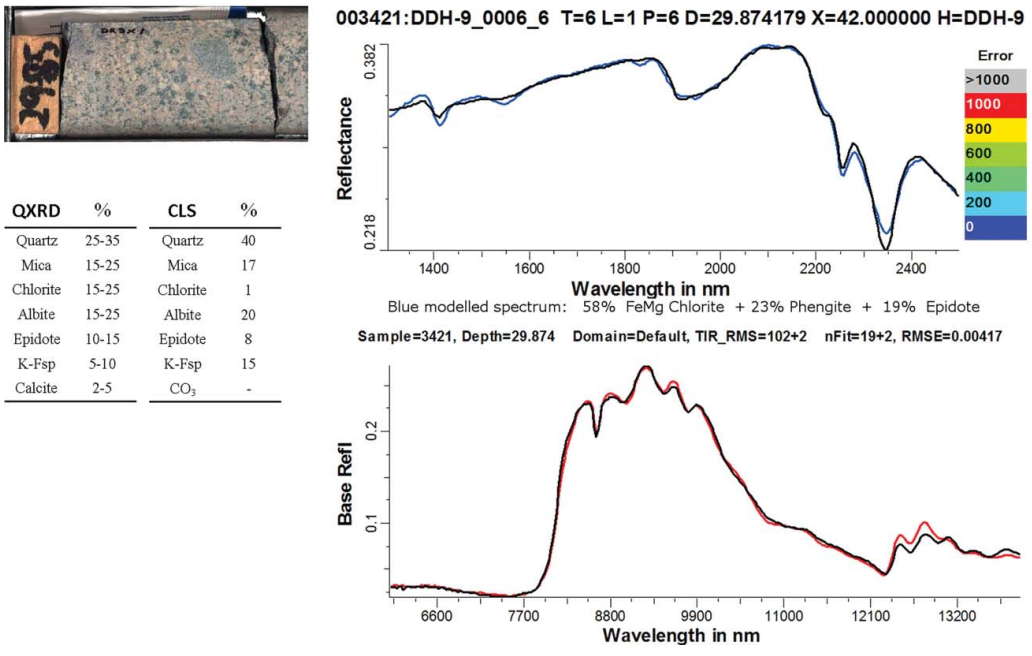

QXRD	%	CLS	%
Quartz	25-35	Quartz	40
Mica	15-25	Mica	17
Chlorite	15-25	Chlorite	1
Albite	15-25	Albite	20
Epidote	10-15	Epidote	8
K-Fsp	5-10	K-Fsp	15
Calcite	2-5	CO_3	-

Figure 9. Example comparison of SWIR and TIR modelled mineral abundances *vs* QXRD abundances. The black lines are the measured spectra while the blue and red lines, respectively, are the modelled spectra. For the SWIR results the nominated mixtures are indicated at the bottom of the upper plot, while for the TIR they are indicated in the table on the left.

appear and epidote is absent. Carbonates occur in both domains in minor abundance.

In addition, to the automatic mineralogical interpretation methods just described, minerals may be targeted with wavelength specific scalars or indices that can map their absorption wavelength (sometimes an indicator of composition) or absorption depth (an indicator of relative abundance). Figure 8 illustrates such a case for the abundance of prehnite [$Ca_2Al_2Si_3O_{10}(OH)_2$] throughout the drill hole.

Both instrument-derived spectra and software-derived mineral interpretations need to be validated. To test the spectroscopic methods quantitative X-ray diffraction analysis (QXRD) was carried out on selected samples. In general, interpreted spectral data do not measure modal mineralogy. However, the results from unmixing spectral data can provide a good guide to the modal mineralogy when the bulk mineralogy is well represented at the surface of clean samples. Of course, when the rock is composed of minerals that are inactive in the spectral region (e.g. quartz in the VNIR–SWIR, and many sulfides in the TIR) the results become less reliable. Examples where we have found our accuracy to be broadly consistent with other published results based on similar spectral measurements are Feely and Christensen (1999), Hamilton and Christensen (2000) and Ramsay and Christensen (1998).

Figure 9 shows a sample at depth 29.88 m from the Dargues Reef drill hole. The unmixing result of the SWIR data suggested chlorite, phengite and epidote as the major components of the spectrum. This components were confirmed by QXRD results showing those minerals in similar fractions in the sample. The comparison between the QXRD and the unmixing result of the TIR spectrum also confirmed the components in regard to the framework silicates (quartz, albite and K-feldspar) and mica. TIR abundance discrepancies are visible for chlorite, epidote and carbonates. Chlorite and epidote are spectrally detected, but estimated in lower abundances. Carbonates are absent from the unmixing results, which is in agreement with a visual interpretation of the spectrum, as there is no spectral evidence. Both diagnostic carbonate features at around 6500 and 11 000 nm are missing, or are extremely weak, so that the unmixing algorithm ignored them for the selected threshold. The weak broad peak at 11 300 nm can be better related to epidote than to a carbonate.

The abundance differences between the QXRD and the spectral results described in the previous paragraph may be explained by the method used for sampling of the rock for QXRD analysis. It is not possible to ensure that exactly the same material from which the spectrum was measured is sampled for XRD. Another equally likely explanation is that the carbonate content was below the detection level as indicated by the QXRD estimate of 2–5%.

Conclusions

The HyLogger-3 is an integrated hardware-software system for the imaging and hyperspectral characterisation of drill cores. Eight such systems have been installed; six in geological surveys in Australia, one at CSIRO in Sydney and one at the University of Chile in Santiago. Capable of a throughput of hundreds of metres per day, the HyLogger-3 targets primarily oxide, hydrous, anhydrous, sulfate, carbonate and phosphate minerals. It acquires continuous, calibrated measurements of spectral reflectance within nominal 10 by 18 mm fields of view. These spectra are processed by a series of automatic and semi-automatic mineralogical unmixing algorithms

along with numerous other interpretation tools provided in The Spectral Geologist (TSG™) software package. Outputs include a wide variety of mineralogical and image products for use by workers in many branches of the earth sciences with the aim of increasing the speed and objectivity of drill core characterisation and mineralogical logging.

Notes

1. 400–2500 nm = 0.4–2.5 μm, 6000–14 500 nm = 6.0–14.5 μm.
2. ENVI: Environment for Visualising Images (http://www.harrisgeospatial.com/).
3. IFOV: Instantaneous Field of View.

Acknowledgements

Initial development of the HyLogging hardware and software systems was made possible by CSIRO and supported by several companies through AMIRA International. Subsequent upgrades to HyLogger-2 and HyLogger-3 capabilities were made possible through CSIRO and the support of the Federal Government's National Collaborative Research Infrastructure Scheme and administered by AuScope Pty Ltd. Further improvements have been possible with the ongoing support of AuScope, CSIRO and all the Australian State and Territory Geological Surveys. All these parties are acknowledged and sincerely thanked for their support.

Disclosure statement

No potential conflict of interest was reported by the authors.

References

Australian Academy of Science. (2012). *Searching the deep earth. A vision for exploration geoscience in Australia*. 43 p. ISBN: 978-0-85847-332-4. Canberra ACT.

Berman, M., Bischof, L., & Huntington, J., (1999). Algorithms and software for the automated identification of minerals using field spectra or hyperspectral imagery: In Proceedings of the 13th International Conference on Applied Geologic Remote Sensing, Vancouver. Volume **1**, 222–232.

Berman, M., Bischof, L., Lagerstrom, R., Guo, Y., Huntington, J., & Mason, P. (2011). *An unmixing algorithm based on a large library of shortwave infrared spectra*. North Ryde NSW: CSIRO Report EP117468.

De Maesschalck, R., Jouan-Rimbaud, D., & Massart, D. L. (2000). The Mahalanobis distance. *Chemometrics and Intelligent Laboratory Systems*, *50*, 1–18.

Duke, E. F. (1994). Near Infrared spectra of muscovite, Tschermak substitution, and metamorphic reaction progress: Implications for remote sensing. *Geology*, *22*, 621–624.

Feely, K. C., & Christensen, P. R. (1999). Quantitative compositional analysis using thermal emission spectroscopy: Application to igneous and metamorphic rocks. *Journal of Geophysical Research*, *104*, No. E10, 24 195–24 210.

Haest, M., Cudahy, T., Laukamp, C., & Gregory, S. (2012a). Quantitative mineralogy from infrared spectroscopic data, Part I. Validation of mineral abundance and composition scripts at the Rocklea Channel Iron Deposit in Western Australia. *Economic Geology*, *107*, 209–228.

Haest, M., Cudahy, T., Laukamp, C., & Gregory, S. (2012b). Quantitative mineralogy from infrared spectroscopic data. Part II. Three-dimensional mineralogical characterization of the Rocklea Channel Iron Deposit, Western Australia. *Economic Geology*, *107*, 229–249

Hamilton, V. E., & Christensen, P. R. (2000). Determining the modal mineralogy of mafic and ultramafic igneous rocks using thermal emission spectroscopy. *Journal of Geophysical Research*, *105*, No. E4, 9717–9733.

Hapke, B. (2012). *Theory of Reflectance and Emittance Spectroscopy* (2nd ed.). Cambridge: Cambridge University Press.

Huntington, J. F., Quigley, M., Yang, K., Roache, T., Young, C., Roberts, I., Whitbourn, L. B., & Mason, P. (2006). A geological overview of HyLogging 18,000 m of core from the Eastern Goldfields of Western Australia. In S. Dominy (Ed.), Proc 6th Int. Mining Geology Conf., Darwin, Australia, 21–23 August 2006 (pp. 45–50). Melbourne Vic: Aus IMM Publication Series No.**6/2006**. ISBN 1 920806 50 4.

Lane, M. D., & Christensen, P. R. (1997). Thermal infrared emission spectroscopy of anhydrous carbonates. *Journal of Geophysical Research*, *102*, 25 581–25 593.

Lawson, C. L., & Hanson, R. J. (1995). *Solving Least Squares Problems. Classics in Applied Mathematics*. Philadelphia: SIAM.

McLachlan, G. J. (1992). *Discriminant Analysis and Statistical Pattern Recognition*. New York: Wiley.

McLeod, R. L., Gabell, A. R., Green, A. A., & Gardavsky, V. (1987). Chlorite infrared spectral data as proximity indicators of volcanic massive sulphide mineralisation, Proc. PACRIM Congress, Gold Coast, Australia, pp. 321–324.

Menke, W. (1989). *Geophysical Data Analysis: Discrete Inverse Theory* (Revised Edition). San Diego, California, Academic Press.

Miller, A. (2002). *Subset Selection in Regression* (2nd ed.). London: Chapman and Hall.

Nocedal, J., & Wright, S. (1999). *Numerical Optimization*. New York: Springer.

Ramsay, M. S., & Christensen, P. R. (1998). Mineral abundance determination: Quantitative deconvolution of thermal emission spectra. *Journal of Geophysical Research*, *103*, No. B1, 577–596.

Reid, W., & Clissold, M. E. (2010). *Linking Drill Core, Field Sample and Airborne Mineralogy: Lachlan Orogen and Broken Hill Examples from the NSW NVCL Node*. Canberra ACT, Australia, 3D Mineral Spectroscopy of the Earth's Skin. The 1st National Virtual Core Library Symposium, July 8–9th 2010, a Topical Symposium of the Australian Earth Science Convention (AESC-2010). Abstract Volume. Page. 22.

Roache, T. J., Walshe, J. L., Huntington, J. F., Quigley, M. A., Yang, Y., Bil, B. W., Blake, K. L., & Hyvarinen, T. (2011). Epidote–clinozoisite as a hyperspectral tool in exploration for Archean gold. *Australian Journal of Earth Sciences*, *58*, 813–822.

Salisbury, J. W., & Walter, L. S. (1989). Thermal infrared (2.5–13.5 μm) spectroscopic remote sensing of igneous rock types on particulate planetary surfaces. *Journal of Geophysical Research*, *94*, 9192–9202.

Salisbury, J. W., Walter, L. S., Vergo, N., & D'Aria, D. M. (1991). *Infrared (2.1–25 μm) Spectra of Minerals*. Baltimore and London: The Johns Hopkins University Press.

Salisbury, J. W., & Wald, A. (1992). The role of volume scattering in reducing spectral contrast of Reststrahlen bands of powdered minerals. *ICARUS*, *96*, 121–129.

Scott, K. M., Yang, K., & Huntington, J. F. (1998). *The application of spectral reflectance studies of chlorites in mineral exploration*. North Ryde NSW: CSIRO Exploration & Mining Report, 545R. AMIRA Project **P435**.

Thompson, J. L., & Salisbury, J. W. (1993). The mid-infrared reflectance of mineral mixtures (7–14 μm). *Remote Sensing of Environment*, *45*, 1–13.

Thompson, A., Scott, K., Huntington, J. F., & Yang, K. (2008). Mapping mineralogy with reflectance spectroscopy: Examples from volcanogenic massive sulphide deposits. In R. Bedell, A. Crosta & E. Grunsky (Eds.), *Reviews in Economic Geology* (Vol. 16, pp. 25–40). Boulder Co: Society of Economic Geologists. ISBN 978-1-934969-13-7.